

HMMoce: An R package for improved geolocation of archival-tagged fishes using a hidden Markov method

Camrin D. Braun^{1,2*}, Benjamin Galuardi^{3,4}, Simon R. Thorrold²

1. Massachusetts Institute of Technology-Woods Hole Oceanographic Institution Joint Program in Oceanography/Applied Ocean Science and Engineering, Cambridge, MA 02139

2. Biology Department, Woods Hole Oceanographic Institution, Woods Hole, MA 02543

3. School of Marine Science and Technology, University of Massachusetts Dartmouth, Fairhaven, MA 02719

4. Greater Atlantic Regional Fisheries Office, National Marine Fisheries Service, National Oceanic and Atmospheric Administration, Gloucester, MA 01930

1 Summary

1. Electronic tagging of marine fishes is commonly achieved with archival tags that rely on light levels and sea surface temperatures to retrospectively estimate movements. However, methodological issues associated with light-level geolocation have constrained meaningful inference to species where it is possible to accurately estimate time of sunrise and sunset. Most studies have largely ignored the oceanographic profiles collected by the tag as a potential way to refine light-level geolocation estimates.
2. Open-source oceanographic measurements and outputs from high-resolution models are increasingly available and accessible. Temperature and depth profiles recorded by electronic tags can be integrated with these empirical data and model outputs to construct likelihoods and improve geolocation estimates.
3. The R package `HMMoce` leverages available tag and oceanographic data to improve position estimates derived from electronic tags using a hidden Markov approach. We illustrate the use of the model and test its performance using example blue and mako shark archival tag data. Model results were validated using independent, known tracks and compared to results from other geolocation approaches.
4. `HMMoce` exhibited as much as 6-fold improvement in pointwise error as compared to traditional light-level geolocation approaches. The results demonstrated the general applicability of `HMMoce` to marine animals, particularly those that do not frequent surface waters during crepuscular periods.

27 **Key words:** satellite telemetry; movement ecology; oceanography; state-space model; behavioral state

28 * Correspondence author. Email: cbraun@whoi.edu

29 **2 Introduction**

30 Electronic archival tags have been widely adopted by ecologists to track movements of wide-ranging species
31 that are difficult to monitor using other techniques. In ocean environments, implanted archival and pop-up
32 satellite archival transmitting (PSAT) tags have proved particularly valuable in the study of life history
33 patterns (e.g. Thorrold et al., 2014), biophysical interactions and habitat use (e.g. Braun et al., 2015b; Lam
34 et al., 2014), horizontal and vertical movements (e.g. Braun et al., 2014; Lam et al., 2016; Werry et al., 2014),
35 and the spatial structure of populations (Skomal et al., 2009; Galuardi et al., 2010; Galuardi and Lam, 2014)
36 in a number of commercially important fishes (Block et al., 2011) and species of conservation concern (Braun
37 et al., 2015a). Yet, tracks provided by electronic tags that rely on light-level geolocation often exhibit large
38 error in daily position estimates (Musyl et al., 2011; Braun et al., 2015b) that may hinder inferences drawn
39 from the tag data. Approaches that provide more certainty in movement estimates derived from light level
40 data (Galuardi and Lam, 2014; Luo et al., 2015) would increase the power of ecological hypotheses tested
41 using tag data.

42 Electronic archival tags typically use light levels to estimate position when it is not possible for the tag to
43 interrogate geo-location satellites (Sibert et al., 2003; Nielsen and Sibert, 2007). Accuracy of geolocation using
44 light levels, however, is limited (± 100 -200 km; $\sim 10,000$ km²) even for surface-oriented species where good light
45 data is available (Wilson et al., 2007; Braun et al., 2015b). While several studies have incorporated ancillary
46 data, including sea surface temperature (Smith and Goodman, 1986; Lam et al., 2010), tidal fluctuation
47 (Pedersen et al., 2008) or ocean heat content (Luo et al., 2015) to help improve geolocation estimates, only
48 one used all data collected from archival tags within a rigorous statistical framework to improve geolocation
49 estimates (Sumner et al., 2009). Although excursions from the photic zone, including diel vertical migration
50 (Neilson et al., 2009) and extended mesopelagic occupation (Skomal et al., 2009) may render light geolocation
51 impossible, the depth-temperature profiles recorded by the tags provide diagnostic oceanographic signatures
52 that can be leveraged to help constrain position (Skomal et al., 2009; Aarestrup et al., 2009).

53 Hidden Markov Models (HMMs) have gained popularity in recent years as a tool for analyzing animal
54 movement data and have been applied to understand movements of a number of organisms (Holzmann
55 et al., 2006; Thygesen et al., 2009; Pedersen et al., 2011). Much of the progress in ocean environments

56 stems from a HMM used to track cod in the North Sea using tidal information (Pedersen et al., 2008). The
57 approach combined a number of desirable features, including inference about the underlying behavioral
58 state of the animal, mobilization of oceanographic data in a spatial likelihood framework (Nielsen et al.,
59 2006), and later incorporated formal treatment of barriers to movement (Pedersen et al., 2011). Generally,
60 the Bayesian HMM approach uses a model of animal movements (e.g. Brownian motion) and a model of
61 observations of the environment (e.g. in situ oceanography) to estimate the posterior distribution of the
62 state (e.g. animal position and behavior). Several R packages exist for analyzing movement data with HMMs,
63 including `ctmm` (Calabrese et al., 2016) and `moveHMM` (Michelot et al., 2016), but none are designed for
64 geolocating marine fishes with archival tag data. An electronic tag manufacturer (Wildlife Computers, Inc.)
65 recently updated their proprietary software (GPE3) to geolocate archival tag data based on light levels and
66 sea surface temperature (SST) in a HMM framework following Pedersen et al. (2008). However, GPE3 is
67 limited by a lack of behavior state-switching dynamics and does not include functionality for non-surface
68 oriented species. GPE3 is also proprietary software that cannot be modified by the user and is limited to
69 tags built by Wildlife Computers.

70 Our primary objective was to build an analysis toolkit to improve geolocation estimates from electronic
71 archival tags deployed on marine animals that alleviates many of the limitations imposed by previous
72 approaches. The new R package `HMMoce` uses available electronic tag data and oceanographic data mined
73 from ocean observing system portals to estimate animal movements, behavior, and residency from uncertain
74 and temporally correlated movement data. We modify and expand a hidden Markov approach (Thygesen
75 et al., 2009; Pedersen et al., 2008, 2011) that, in addition to estimating animal movements, allows behavior
76 state estimation and provides information about the posterior distribution of the modeled states that can
77 be used as a residency metric (Pedersen et al., 2011). The modeling framework we developed is sufficiently
78 flexible to accommodate other tag types and animal movement questions, can be applied in any geographic
79 location, and benefits from the transparency of a widely-used open source platform. Here we describe the
80 model framework and demonstrate its applicability using example data. For specific details on package use
81 and functions and a full tutorial with an example dataset, please refer to the package and its accompanying
82 vignette, available on CRAN.

3 Overview of HMMocean

3.1 Model formulation

We present a process-based approach to estimate residency and behavior from movement data collected with electronic archival tags. The logic of this approach involves calculating gridded observation likelihoods at each time point based on tag and environmental data, forming the state-space model, estimating model parameters and model selection and interpretation. The application of grids to explicitly resolve space is a key component that allows state estimation (location and behavior, in this case) to be supplemented by or based entirely on environmental data (e.g. temperature at depth). The details of the discretized grid HMM approach are thoroughly explained elsewhere (e.g. Thygesen et al., 2009; Pedersen et al., 2011). A detailed methodology for our approach can be found in the supplement.

Briefly, observation-based likelihoods (Eq. S1) were derived from in situ SST (Eq. S2), light-based longitude and depth-temperature profile data (Eqs. S3, S4, S5) collected by the tags using five separate likelihood calculations: 1) An SST likelihood (Eq. S2) was generated for tag-based SST values integrated according to an error term ($\pm 1\%$, based on tag sensor accuracy) and compared to remotely-sensed SST from daily, optimally-interpolated SST fields (OI-SST, 0.25° resolution; Banzon et al., 2016). 2) Light-based longitude likelihood was derived using estimates of longitude from GPE2 software (Wildlife Computers, Inc.), which facilitated visual checking of light curves. Depth-temperature profiles recorded by the tag were compared to 3) monthly climatological mean depth-temperature data from the World Ocean Atlas 2013 (WOA, 0.25° resolution; Locarnini et al., 2013) and 4) daily reanalysis model depth-temperature products from the HYbrid Coordinate Ocean Model (HYCOM, 0.08° resolution; Chassignet et al., 2007) at standard depth levels available in these products (Eq. S5). Individual likelihood surfaces for each depth level were then combined for an overall profile likelihood at that time point (Eq. S6). 5) Ocean Heat Content (OHC, Eq. S3) was obtained by integrating the heat content of the water column above the minimum daily temperature recorded by the tag for both the tag profiles and HYCOM fields (Eq. S4; Luo et al., 2015). Start and end locations were considered known in all cases and model runs.

The resulting observation likelihoods (in various combinations; Eq. S1) were used in a two-step Bayesian state-space approach to estimate the posterior distribution of the state (in this case, a joint probability distribution of location and behavior at each time point). Probability distributions were first calculated forward in time using alternating time and data updates of the current state estimate using a HMM filter (for a detailed methodology of the HMM filter see Appendix 2 in Pedersen et al., 2011). The filter recursions

113 also returned a likelihood measure indicating how well the model fit the data, which facilitated calculating
114 model parameters (e.g. behavior state-switching probabilities). In Bayesian statistics, the maximum a priori
115 (MAP) estimate of the model parameters is typically used to calculate the posteriors; however, in practice,
116 ample a priori information is rarely available and maximum likelihood (ML) estimates are often very similar
117 to MAP estimates (Jonsen et al., 2005). Thus, we implemented recent advances by Woillez et al. (2016) that
118 further exploited the discretization of space in this model by employing a joint ML estimation of all model
119 parameters using an iterative Expectation-Maximization framework (Supp. 1.4.1).

120 Model selection in this context would typically use Bayesian Information criterion (BIC), but this approach
121 requires approximation that imposes restrictions on the priors. Instead, we used Akaike's Information criterion
122 (AIC) for model selection following Pedersen et al. (2011). The HMM smoother recursion was the final step
123 that worked backwards in time using filtered state estimates and all available observation data to determine
124 smoothed state estimates. This step provided the time marginal of the probability distributions based on
125 observations (posterior distributions).

126 Results from the final smoothing step represent the posterior distribution of each state over time. Distributions
127 are summed for each behavior state and time step to determine the most likely behavior state through time.
128 `HMMoce` can calculate the mean or mode of the posterior distribution grid, at each time step, to estimate the
129 animal's position. The posteriors can be further analyzed for additional inference including uncertainty and
130 residency. A residency distribution (RD) is conceptually similar to the utilization distribution (UD), but
131 the concept of UD (and other space-use metrics) is often vaguely defined (Royle and Dorazio, 2008). In this
132 case, RD is interpreted as the estimate of the time spent in a given space within a time interval (see Eq. 5 in
133 Pedersen et al., 2011).

134 **3.2 Computational improvements and requirements**

135 While the basic framework of `HMMoce` was based on previous work (Pedersen et al., 2008; Thygesen et al.,
136 2009; Pedersen et al., 2011), several improvements were made to accommodate user needs. We focused several
137 enhancements on improving computation efficiency, which was a limitation of previous techniques (`SPHMM`
138 code for R; Pedersen et al., 2011). Image processing routines replaced sparse matrix convolution yielding
139 orders of magnitude improvements in computation time, particularly for large, high-resolution grids that
140 characterize geolocation approaches for highly migratory species. In addition, all likelihood routines (except
141 simple light-based likelihood calculations) were parallelized, yielding marked performance improvements,
142 particularly for likelihoods comparing 3D depth-temperature profiles to high-resolution 3D HYCOM grids.

143 Despite these improvements, `HMMoce` remains relatively computationally intensive; however, cloud computing
144 is becoming more inexpensive and accessible to a broad user group. The `HMMoce` package includes a vignette
145 demonstrating simple plug and play functionality for the model using Amazon Web Services’s computational
146 resources and an associated machine image containing RStudio Server and all the required dependencies for
147 running `HMMoce` with user-provided tag data.

148 4 Case study: pelagic shark movements

149 To illustrate the application of `HMMoce`, we analyzed tag data from three blue sharks (*Prionace glauca*) and
150 one shortfin mako (*Isurus oxyrinchus*) that were double-tagged with satellite-linked radio telemetry tags
151 (Wildlife Computers finmount SPOT5 tags) and PSAT tags (Table 1). Full tagging methods are provided in
152 the supplement. We considered the resulting Argos-based tracks as “known” because errors on geolocation
153 estimates from the SPOT tags are much lower (typically < 10 km; Witt et al., 2010; Patterson et al., 2010)
154 than PSAT-based outputs (> 50 km; Winship et al., 2012). The PSAT tags were deployed for an average of
155 150 days (range 107-180) in the northwest Atlantic with overall movements of 5403-12122 km. The PSAT
156 data contained depth-temperature profiles for 53-72% of days at liberty and SPOT locations were recorded
157 for 72-96% of deployment days (Table 1).

158 Blue sharks made frequent dives to the mesopelagic zone (~600-800m, max 680-1688m) but also frequented
159 the surface-air interface where the PSAT tags collected good quality light and SST data (94-100% deployment
160 days with light, 82-92% SST)(Fig. 1). The mako occupied a restricted area (~200 km latitudinal distance)
161 near Cape Hatteras during the winter months and spent relatively little far from the edge of the continental
162 shelf compared to the more nomadic blue sharks. The mako also had high quality light and SST data (96%
163 and 69%, respectively) while regularly diving shallower than the blue sharks (~400m). Consistent exposure of
164 the dorsal fin allowed the SPOT tag to acquire Argos positions throughout the duration of each deployment
165 (Table 1).

166 We calculated movements of the sharks from PSAT tag data using three modeling approaches that are
167 currently available (Ukfstt, Trackit, GPE3) and `HMMoce` (Supp. 1.6). Results for the mako are shown in
168 the main text (Fig. 2), and blue shark figures are provided in the supplement (Figs. S2, S3, S4). In
169 general, `HMMoce` and GPE3 produced the most accurate tracks while those from Ukfstt and Trackit were often
170 unrealistic with errors as high as >1300 km (Table 2). For 3 of 4 individuals, `HMMoce` tracks had the lowest
171 pointwise error and correspondingly lowest root-mean-square error (RMSE) values. For the fourth individual
172 (blue shark 141259), the mean error and RMSE in latitude for GPE3 output was lower than `HMMoce`, which had

173 a lower RMSE in longitude. The traditional approaches (light only, Trackit; light and SST, Uksfst) yielded
174 much larger error than **HMMoce** in all cases and only one Trackit output (blue shark 141254 without SST)
175 exhibited marginally smaller error than GPE3 (with SST). In 3 of 4 cases, **HMMoce** demonstrated the best
176 fitting model by leveraging either OHC (n=1) or HYCOM profiles (n=2) (Table 2) in addition to light-based
177 longitude and SST data used in the other geolocation approaches. The movements of blue shark 141259, in
178 which the **HMMoce** model did not use profile-based observations to build the final estimated track, included
179 time in both dynamic Gulf Stream water and the more homogenous Sargasso Sea. It proved difficult in
180 both areas to match water column profiles recorded by the tag (or integrated OHC) with an accurate and
181 constrained position in the climatological (WOA) or model-based (HYCOM) oceanographic data (Fig. S5).

182 While **HMMoce** was designed to improve geolocation estimates for all tagged marine organisms, the main
183 impetus for the work was to fulfill a need for improving track estimates in cases where light and SST data
184 were lacking due to minimal surface occupation. We tested the ability of **HMMoce** to recover accurate tracks
185 with only limited light-level data by randomly removing (using `sample` in base R, without replacement) 75%
186 and 50% of deployment days with adequate light and SST data, respectively, from the shark PSAT data while
187 keeping the depth-temperature profile data for these days. The removals approximated PSAT data quality
188 typical of swordfish tag deployments in the Atlantic Ocean due to crepuscular diving behavior and light
189 avoidance (Braun et al., 2015a; Neilson et al., 2009). The data removal experiment (Fig. 1) demonstrated
190 the power of incorporating the depth dimension in likelihood calculations when light and/or SST data is
191 poor. In all 4 cases, **HMMoce** estimated tracks with lower mean error than corresponding GPE3 results (Table
192 2), but model selection favored including depth-temperature profile information in only 2 of 4 final models.
193 Error in the removal experiment for **HMMoce** was only marginally higher as compared to the full dataset for 3
194 of 4 individuals (Table 2).

195 Both GPE3 and **HMMoce** provide estimated residency distributions (RD; a form of utilization distribution)
196 (Pedersen et al., 2011). However, only **HMMoce** incorporates a state-switching component that facilitates
197 explicit modeling of distinct animal behaviors (Fig. 3). The state-switching is governed by movement kernels
198 (based on speed) and probability of switching between states is calculated by the EM algorithm (Table S1).
199 For the mako, the RDs indicated areas of core use focused largely where resident behavior was most probable.
200 The RD for the migratory state showed the offshore movement to the SE into the Gulf Stream region before
201 the fish returned to the shelf break and moved SW toward Cape Hatteras. The most notable features of the
202 migratory RD are the overlap areas where the fish transitioned from migratory to resident behaviors (Fig. 4).

5 Conclusions

We present a flexible, customizable and transparent HMM framework that may be applied to nearly any marine species utilizing electronic archival tags through a novel use of oceanographic data. Tests of the model demonstrated that `HMMoce` is a valuable tool for estimating movements from low quality PSAT data through consideration of the vertical structure of the water column in the state estimation. This can be especially beneficial for tag data that is lacking adequate light-level data or other measurements.

For further development, we anticipate several improvements to the `HMMoce` package. Current priorities include support for other tag types, direct versus derived use of light data, and additional algorithms (e.g. Viterbi) to calculate the most probable track (Pedersen et al., 2011). Behavior state estimation could be expanded to include advection or modified to update probability with respect to environmental data (Patterson et al., 2009).

We anticipate user feedback will help prioritize further improvements, and we welcome bug reports, feedback, and suggestions for the development of `HMMoce` via our Github repository <https://github.com/camrinbraun/HMMoce>. Additional usage information, including an example dataset and a tutorial for using `HMMoce` on Amazon Web Services, can be found by installing `HMMoce` in R (`install.packages("HMMoce")`) and accessing the package vignette.

6 Acknowledgements

We thank P. Gaube, M. Kaplan, D. McGillicuddy and A. Solow for helpful discussions during model development. We thank M. Pedersen for inspiration and previous work on model development. This work was funded by awards to C. Braun from the Martin Family Society of Fellows for Sustainability Fellowship at the Massachusetts Institute of Technology, the Grassle Fellowship and Ocean Venture Fund at the Woods Hole Oceanographic Institution, and the NASA Earth and Space Science Fellowship. Computational support was provided by the AWS Cloud Credits for Research program.

Funding for the development of HYCOM has been provided by the National Ocean Partnership Program and the Office of Naval Research. Data assimilative products using HYCOM are funded by the U.S. Navy. Computer time was made available by the DoD High Performance Computing Modernization Program. The output is publicly available at <http://hycom.org>.

All tagging protocols were performed in accordance with the Woods Hole Oceanographic Institution's Animal

231 Care and Use Committee (IACUC) protocol #BI23112.

232 **7 Data accessibility**

233 All code mentioned here is available in the `HMMoce` package for R hosted on CRAN. The development version of
234 the package is available on GitHub at <https://github.com/camrinbraun/HMMoce>. Supporting data (e.g. shark
235 satellite tag data) is distributed with the package from both sources.

236 **8 Author contributions**

237 CDB and BG conceived the project and developed the package. CDB and SRT collected the data. All
238 co-authors wrote the manuscript, assisted with edits and approve publication.

239 **9 Figure captions**

240 Figure 1. Example blue shark data demonstrating the deployment days with [A] light, [B] sea surface
241 temperature and [C] depth-temperature profile data used as the observation portion of the HMM. Full (F)
242 and removal (R) datasets for light and SST are shown [A,B].

243 Figure 2. Calculated tracks for mako shark 141257 using the 4 different geolocation approaches (Ukfsst,
244 purple; Trackit, blue; GPE3, green; `HMMoce`, yellow) compared to the “known” Argos-based track (red, black
245 crosses). Latitudinal and longitudinal estimates through time are shown in panels B and C, respectively.
246 Lines appear broken when a resulting track is missing daily data.

247 Figure 3. Movements (A) and behavior (B) calculated using `HMMoce` for mako 141257. The tagged individual
248 is considered resident where probability of residency is greater than 0.5 (grey points and bars in panels A
249 and B, respectively). Green and red points indicate tag and pop-up location respectively. Black line follows
250 predicted daily locations of tagged shark.

251 Figure 4. Residency distributions for the overall `HMMoce` modeled movements (A) and for individual behavior
252 states (B, C). Shaded circles indicate residency behavior, white circles indicate migratory behavior, green
253 triangle is tagging location and red triangle is pop-up location. Residency distributions show the expected
254 proportion of time spent in various grid cells over the course of tag deployment.

Table 1: Tagging summary for double-tagged blue (BSH) and shortfin mako (MKO) sharks used in this study. PDT, Light, SST and SPOT = percent of deployment period with depth-temperature profile (PDT), light and sea surface temperature (SST) data from the PSAT tag and percent of deployment period with Argos-based positions (SPOT), respectively.

Species	Tag ID	Start Date	End Date	Duration (d)	PDT (%)	Light (%)	SST (%)	SPOT (%)
BSH	141254	2015-10-21	2016-02-05	107	72	100	92	96
BSH	141256	2015-10-13	2016-02-24	134	66	94	88	87
BSH	141259	2015-10-13	2016-04-10	180	53	94	82	85
MKO	141257	2015-10-15	2016-04-12	180	58	96	69	72

Table 2: Validation metrics for double-tagged blue (BSH) and shortfin mako (MKO) shark tracks estimated using HMMoce, GPE3, Trackit (TI) and Uksst. Reported error values (mean, sd, median, range) are pointwise distance calculations (mean great circle distance) from known positions (km). Root-mean-square errors (RMSE) are Lat, Long (degrees). HMMoce.r and GPE3.r indicate fit metrics for data removal experiments in which 75% of daily light and 50% of daily SST data was randomly removed. Input indicates input data type: light (L), SST (S), ocean heat content (O), World Ocean Atlas profiles (W) and HYCOM profiles (H). All runs were performed on a 0.08° grid with fixed migratory speed of 2 m/s (except 141259 used 4 m/s).

Species	Tag ID	Type	Mean (SD)	Median	Range	RMSE	Input
BSH	141254	HMMoce	117.4(96.7)	92.4	0.5-443.6	1.21, 0.81	LSO
		GPE3	175.8(117.1)	164.3	3.2-424.7	1.4, 1.64	LS
		TI	162.3(71.6)	158.2	1-328.2	0.97, 1.65	L
		KF	179.5(99.5)	178.5	1-435.2	1.29, 1.24	L
		HMMoce.r	131.2(96.2)	101.9	0.5-440.5	1.23, 1.01	LS
		GPE3.r	157.6(100.6)	143.5	1.4-408.9	1.25, 1.44	LS
BSH	141256	HMMoce	83.8(63)	63.7	4.9-297.4	0.52, 0.93	LSH
		GPE3	84.9(68.8)	66.9	5.9-345	0.66, 0.89	LS
		TI	474.2(244.1)	459.9	0-854.3	1.98, 4.84	L
		KF	192.7(152.4)	172.6	0-699.8	1.35, 0.65	L
		HMMoce.r	93.4(57.8)	79.1	4.2-286	0.59, 0.92	LSH
		GPE3.r	423.5(432)	197.8	2.1-1394	4.25, 3.96	LS
BSH	141259	HMMoce	179.4(126)	150.3	4.4-575.2	1.79, 1	LS
		GPE3	158.1(109.6)	139.5	4.9-434.5	1.44, 1.17	LS
		TI	367.5(239.1)	291.4	2.4-861.5	3.3, 2.36	L
		KF	245.8(225.5)	194.5	1.7-1078.7	2.31, 0.88	L
		HMMoce.r	183.3(132.2)	140.5	4.4-560.5	1.9, 0.88	LS
		GPE3.r	198(129.5)	162.0	6.1-625.8	1.61, 1.77	LS
MKO	141257	HMMoce	99.8(90.7)	66.8	3.8-426.9	0.92, 0.99	LSH
		GPE3	151.1(161.1)	93.0	6.8-675.2	0.65, 2.38	LS
		TI	462.6(347.7)	320.5	0-1332.7	4.6, 2.79	L
		KF	220.4(151.2)	173.7	0-614.6	1.3, 1.32	L
		HMMoce.r	157.9(128.2)	119.1	3.8-494.4	1.05, 1.92	LSH
		GPE3.r	182.3(171.8)	136.4	0.3-711.2	0.88, 2.62	LS

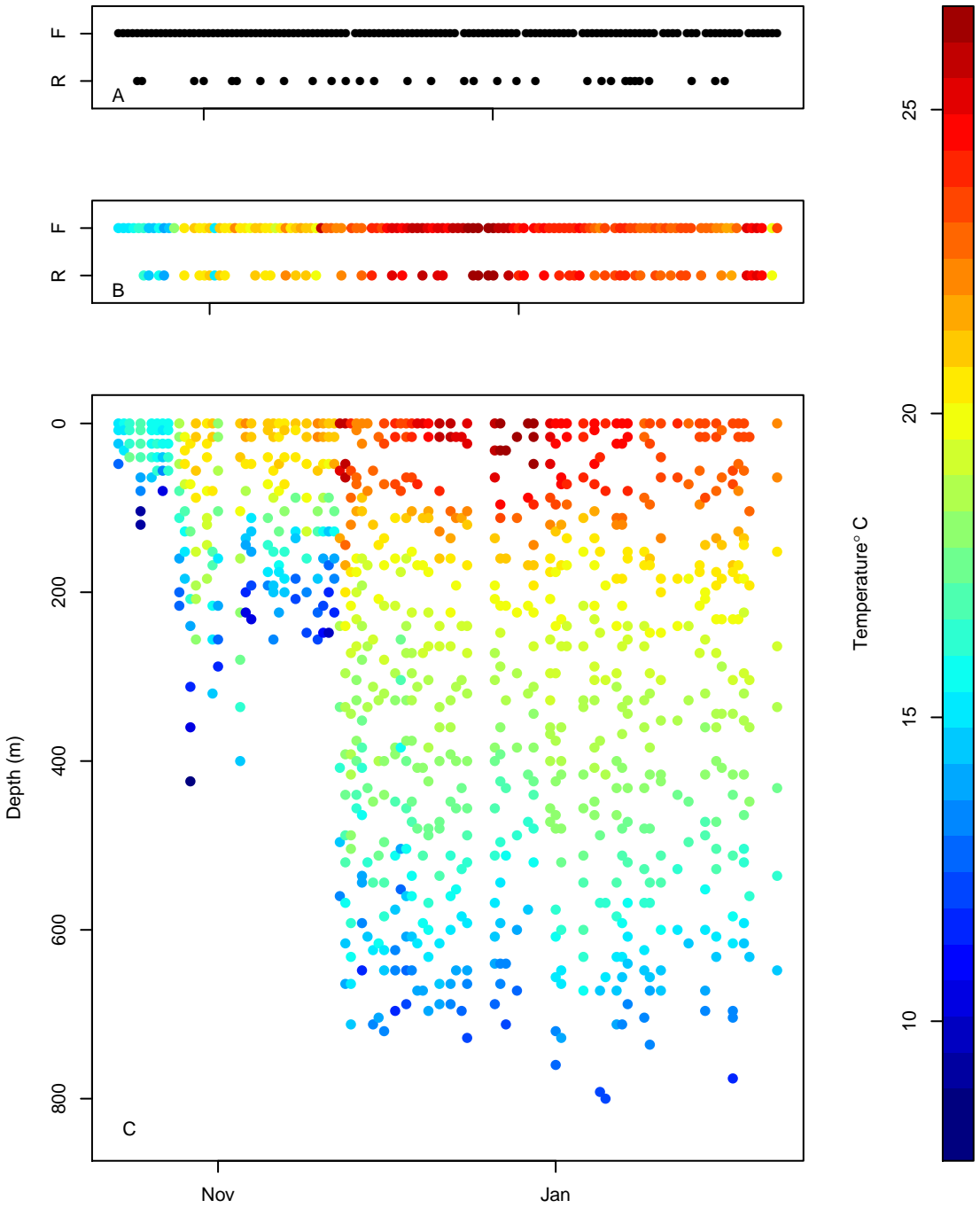
References

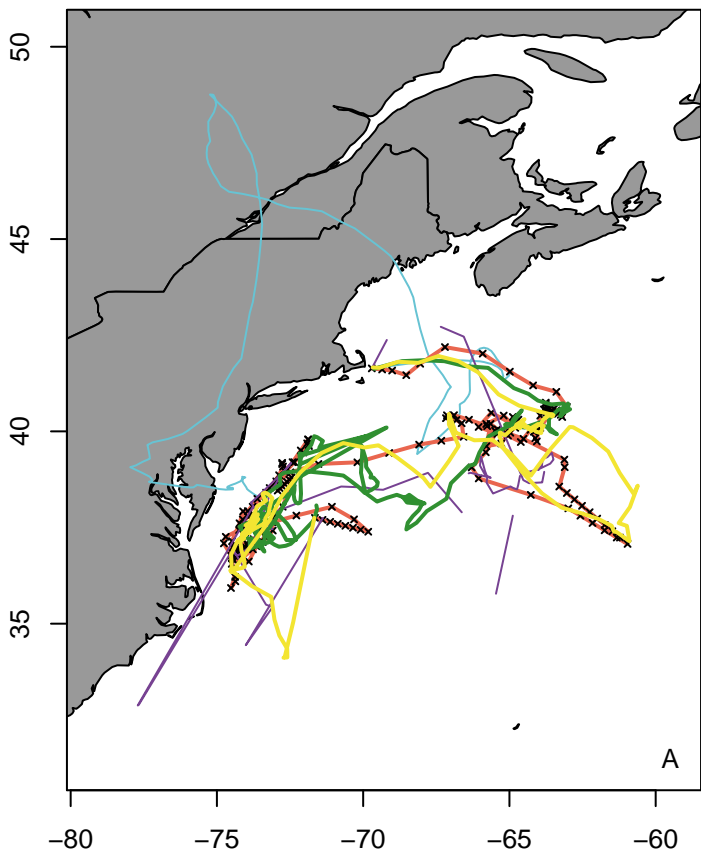
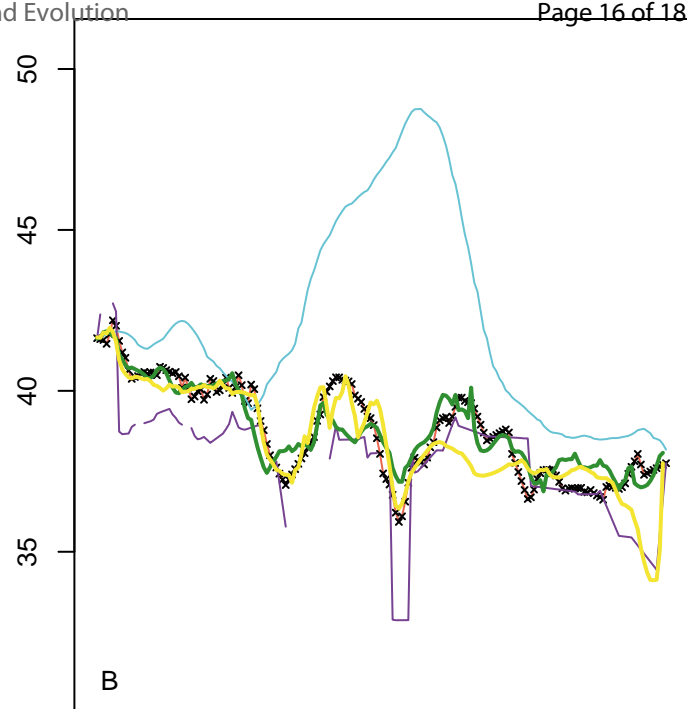
- 255
256 Aarestrup, K., Okland, F., Hansen, M. M., Righton, D., Gargan, P., Castonguay, M., Bernatchez, L., Howey,
257 P., Sparholt, H., Pedersen, M. I., and McKinley, R. S. (2009). Oceanic Spawning Migration of the European
258 Eel (*Anguilla anguilla*). *Science*, 325(5948):1660–1660.
- 259 Banzon, V., Smith, T. M., Mike Chin, T., Liu, C., and Hankins, W. (2016). A long-term record of blended
260 satellite and in situ sea-surface temperature for climate monitoring, modeling and environmental studies.
261 *Earth System Science Data*, 8(1):165–176.
- 262 Block, B. A., Jonsen, I. D., Jorgensen, S. J., Winship, A. J., Shaffer, S. A., Bograd, S. J., Hazen, E. L., Foley,
263 D. G., Breed, G. A., and Harrison, A. L. (2011). Tracking apex marine predator movements in a dynamic
264 ocean. *Nature*, 475(7354):86–90.
- 265 Braun, C. D., Kaplan, M. B., Horodysky, A. Z., and Llopiz, J. K. (2015a). Satellite telemetry reveals physical
266 processes driving billfish behavior. *Animal Biotelemetry*, 3(1):2.
- 267 Braun, C. D., Skomal, G. B., Thorrold, S. R., and Berumen, M. L. (2014). Diving Behavior of the Reef
268 Manta Ray Links Coral Reefs with Adjacent Deep Pelagic Habitats. *PLoS One*, 9(2):e88170.
- 269 Braun, C. D., Skomal, G. B., Thorrold, S. R., and Berumen, M. L. (2015b). Movements of the reef manta ray
270 (*Manta alfredi*) in the Red Sea using satellite and acoustic telemetry. *Marine Biology*, 162(12):2351–2362.
- 271 Calabrese, J. M., Fleming, C. H., Gurarie, E., and Freckleton, R. (2016). Ctmm: an R Package for Analyzing
272 Animal Relocation Data As a Continuous-Time Stochastic Process. *Methods in Ecology and Evolution*,
273 7(9):1124–1132.
- 274 Chassignet, E. P., Hurlburt, H. E., Smedstad, O. M., Halliwell, G. R., Hogan, P. J., Wallcraft, A. J., Baraille,
275 R., and Bleck, R. (2007). The HYCOM (HYbrid Coordinate Ocean Model) data assimilative system.
276 *Journal of Marine Systems*, 65(1-4 SPEC. ISS.):60–83.
- 277 Galuardi, B. and Lam, C. H. T. (2014). Chapter Nineteen - Telemetry Analysis of Highly Migratory Species.
278 pages 447–476.
- 279 Galuardi, B., Royer, F., Golet, W., Logan, J., Neilson, J., and Lutcavage, M. (2010). Complex migration routes
280 of Atlantic bluefin tuna (*Thunnus thynnus*) question current population structure paradigm. *Canadian*
281 *Journal of Fisheries and Aquatic Sciences*, 67(6):966–976.
- 282 Holzmann, H., Munk, A., Suster, M., and Zucchini, W. (2006). Hidden Markov models for circular and
283 linear-circular time series. *Environmental and Ecological Statistics*, 13(3):325–347.

- 284 Jonsen, I. D., Flemmings, J. M., and Myers, R. a. (2005). Robust State – Space Modeling of Animal Movement
285 Data. *Ecology*, 86(11):2874–2880.
- 286 Lam, C. H., Galuardi, B., and Lutcavage, M. E. (2014). Movements and oceanographic associations of bigeye
287 tuna (*Thunnus obesus*) in the Northwest Atlantic. *Canadian Journal of Fisheries and Aquatic Sciences*,
288 1543(September 2013):1–15.
- 289 Lam, C. H., Galuardi, B., Mendillo, A., Chandler, E., and Lutcavage, M. E. (2016). Sailfish migrations
290 connect productive coastal areas in the West Atlantic Ocean. *Scientific Reports*, 6(August):38163.
- 291 Lam, C. H., Nielsen, A., and Sibert, J. R. (2010). Incorporating sea-surface temperature to the light-based
292 geolocation model TrackIt. *Marine Ecology Progress Series*, 419:71–84.
- 293 Locarnini, R. A., Mishonov, A. V., Antonov, J. I., Boyer, T. P., Garcia, H. E., Baranova, O. K., Zweng,
294 M. M., Paver, C. R., Reagan, J. R., and Johnson, D. R. (2013). World Ocean Atlas 2013, Volume 1:
295 Temperature. *NOAA Atlas NESDIS*, 73:40.
- 296 Luo, J., Ault, J. S., Shay, L. K., Hoolihan, J. P., Prince, E. D., Brown, C. a., and Rooker, J. R. (2015). Ocean
297 Heat Content Reveals Secrets of Fish Migrations. *Plos One*, 10(10):e0141101.
- 298 Michelot, T., Langrock, R., and Patterson, T. A. (2016). moveHMM: An R package for the statistical
299 modelling of animal movement data using hidden Markov models. *Methods in Ecology and Evolution*,
300 7(11):1308–1315.
- 301 Musyl, M. K., Domeier, M. L., Nasby-Lucas, N., Brill, R. W., McNaughton, L. M., Swimmer, J. Y., Lutcavage,
302 M. S., Wilson, S. G., Galuardi, B., and Liddle, J. B. (2011). Performance of pop-up satellite archival tags.
303 *Marine Ecology Progress Series*.
- 304 Neilson, J. D., Smith, S., Royer, F., Paul, S. D., Porter, J. M., and Lutcavage, M. (2009). Investigations of
305 horizontal movements of Atlantic swordfish using pop-up satellite archival tags. In *Tagging and tracking of*
306 *marine animals with electronic devices*, pages 145–159. Springer.
- 307 Nielsen, A., Bigelow, K. A., Musyl, M. K., and Sibert, J. R. (2006). Improving light-based geolocation by
308 including sea surface temperature. *Fisheries Oceanography*, 15(4):314–325.
- 309 Nielsen, A. and Sibert, J. R. (2007). State–space model for light-based tracking of marine animals. *Canadian*
310 *Journal of Fisheries and Aquatic Sciences*, 64(8):1055–1068.

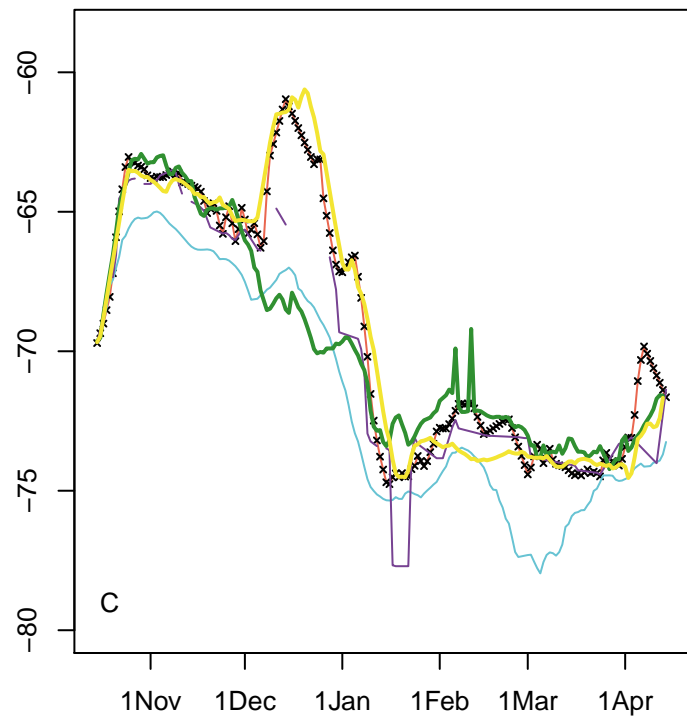
- 311 Patterson, T. A., Basson, M., Bravington, M. V., and Gunn, J. S. (2009). Classifying movement behaviour in
312 relation to environmental conditions using hidden Markov models. *Journal of Animal Ecology*, 78(6):1113–
313 1123.
- 314 Patterson, T. A., McConnell, B. J., Fedak, M. A., Bravington, M. V., and Hindell, M. A. (2010). Using
315 GPS data to evaluate the accuracy of state-space methods for correction of Argos satellite telemetry error.
316 *Ecology*, 91(1):273–285.
- 317 Pedersen, M., Berg, C., Thygesen, U., Nielsen, a., and Madsen, H. (2011). Estimation methods for nonlinear
318 state-space models in ecology. *Ecological Modelling*, 222(8):1394–1400.
- 319 Pedersen, M. W., Righton, D., Thygesen, U. H., Andersen, K. H., and Madsen, H. (2008). Geolocation of
320 North Sea cod (*Gadus morhua*) using hidden Markov models and behavioural switching. *Canadian Journal*
321 *of Fisheries and Aquatic Sciences*, 65(11):2367–2377.
- 322 Royle, J. A. and Dorazio, R. M. (2008). *Hierarchical modeling and inference in ecology: the analysis of data*
323 *from populations, metapopulations and communities*. Academic Press.
- 324 Sibert, J. R., Musyl, M. K., and Brill, R. W. (2003). Horizontal movements of bigeye tuna (*Thunnus*
325 *obesus*) near Hawaii determined by Kalman filter analysis of archival tagging data. *Fisheries Oceanography*,
326 12(3):141–151.
- 327 Skomal, G. B., Zeeman, S. I., Chisholm, J. H., Summers, E. L., Walsh, H. J., McMahon, K. W., and Thorrold,
328 S. R. (2009). Transequatorial migrations by basking sharks in the western Atlantic Ocean. *Current Biology*,
329 19(12):1019–1022.
- 330 Smith, P. and Goodman, D. (1986). *Determining fish movements from an "archival" tag: precision of*
331 *geographical positions made from a time series of swimming temperature and depth*. US Department
332 of Commerce, National Oceanic and Atmospheric Administration, National Marine Fisheries Service,
333 Southwest Fisheries Center.
- 334 Sumner, M. D., Wotherspoon, S. J., and Hindell, M. A. (2009). Bayesian estimation of animal movement
335 from archival and satellite tags. *PLoS One*, 4(10):e7324.
- 336 Thorrold, S. R., Afonso, P., Fontes, J., Braun, C. D., Skomal, G. B., and Berumen, M. L. (2014). Extreme
337 diving behavior in devil rays link surface waters and the deep ocean. *Nature Communications*, 5(4274).
- 338 Thygesen, U. H., Pedersen, M. W., and Madsen, H. (2009). Geolocating Fish Using Hidden Markov Models
339 and Data Storage Tags. *Tagging and Tracking of Marine Animals with Electronic Devices*, 9:23–34.

- 340 Werry, J. M., Planes, S., Berumen, M. L., Lee, K. A., Braun, C. D., and Clua, E. (2014). Reef-Fidelity and
341 Migration of Tiger Sharks, *Galeocerdo cuvier*, across the Coral Sea. *PLoS One*, 9(1):e83249.
- 342 Wilson, S. G., Stewart, B. S., Polovina, J. J., Meekan, M. G., Stevens, J. D., and Galuardi, B. (2007). Accuracy
343 and precision of archival tag data: a multiple-tagging study conducted on a whale shark (*Rhincodon typus*)
344 in the Indian Ocean. *Fisheries Oceanography*, 16(6):547–554.
- 345 Winship, A. J., Jorgensen, S. J., Shaffer, S. a., Jonsen, I. D., Robinson, P. W., Costa, D. P., and Block,
346 B. a. (2012). State-space framework for estimating measurement error from double-tagging telemetry
347 experiments. *Methods in Ecology and Evolution*, 3(2):291–302.
- 348 Witt, M. J., Åkesson, S., Broderick, A. C., Coyne, M. S., Ellick, J., Formia, A., Hays, G. C., Luschi, P., Stroud,
349 S., and Godley, B. J. (2010). Assessing accuracy and utility of satellite-tracking data using Argos-linked
350 Fastloc-GPS. *Animal behaviour*, 80(3):571.
- 351 Woillez, M., Fablet, R., Ngo, T. T., Lalire, M., Lazure, P., and de Pontual, H. (2016). A HMM-based model
352 to geolocate pelagic fish from high-resolution individual temperature and depth histories: European sea
353 bass as a case study. *Ecological Modelling*, 321:10–22.

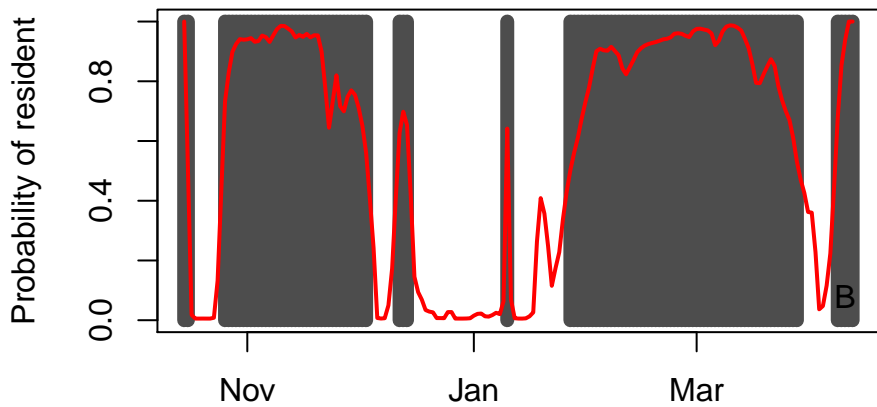
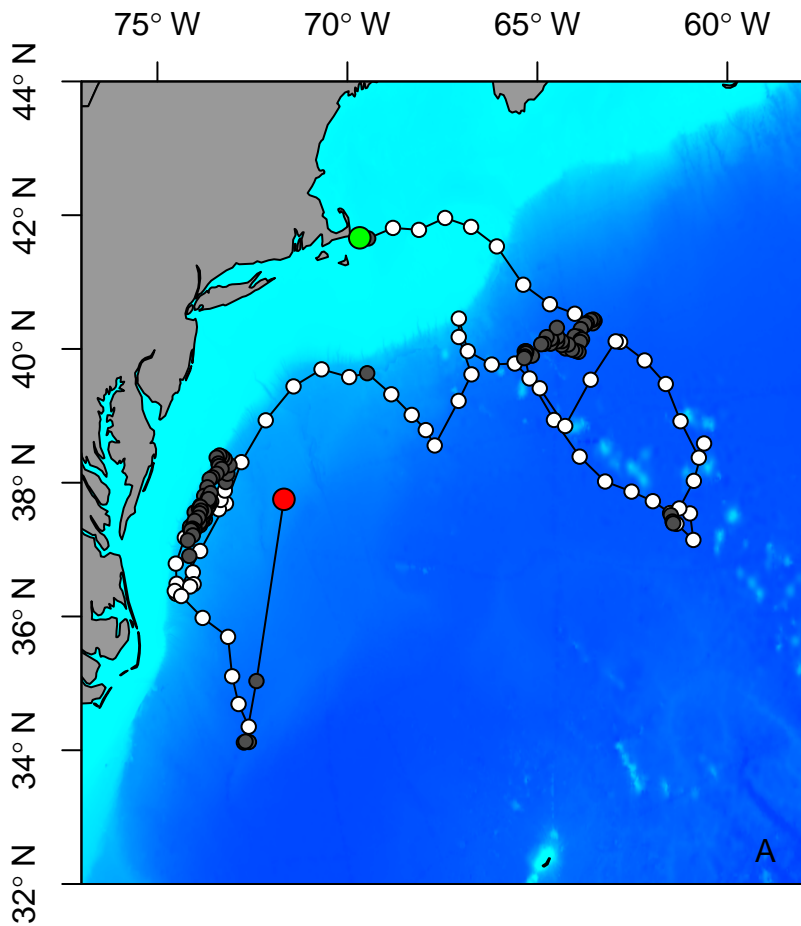


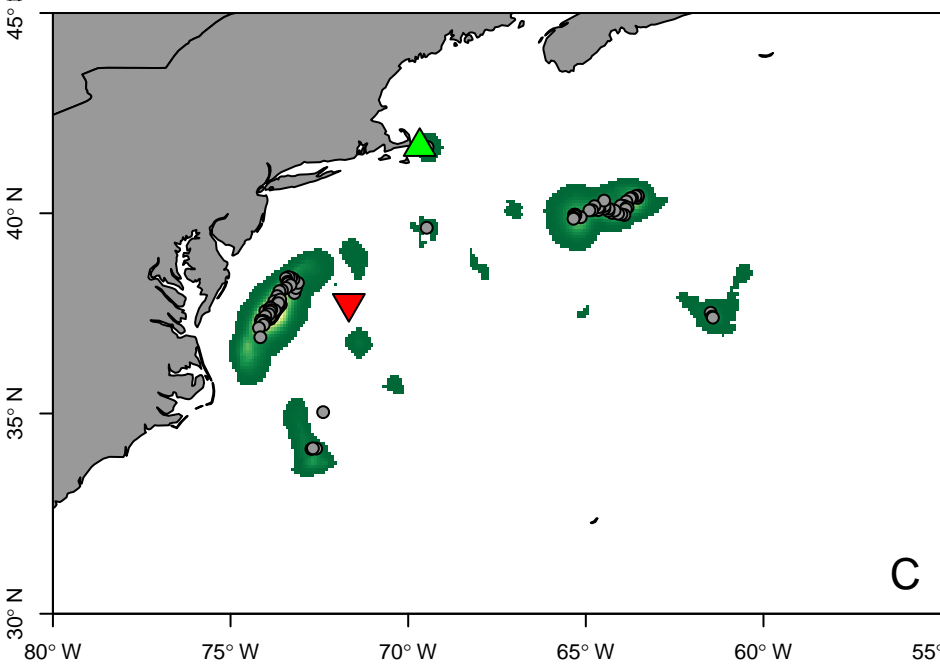
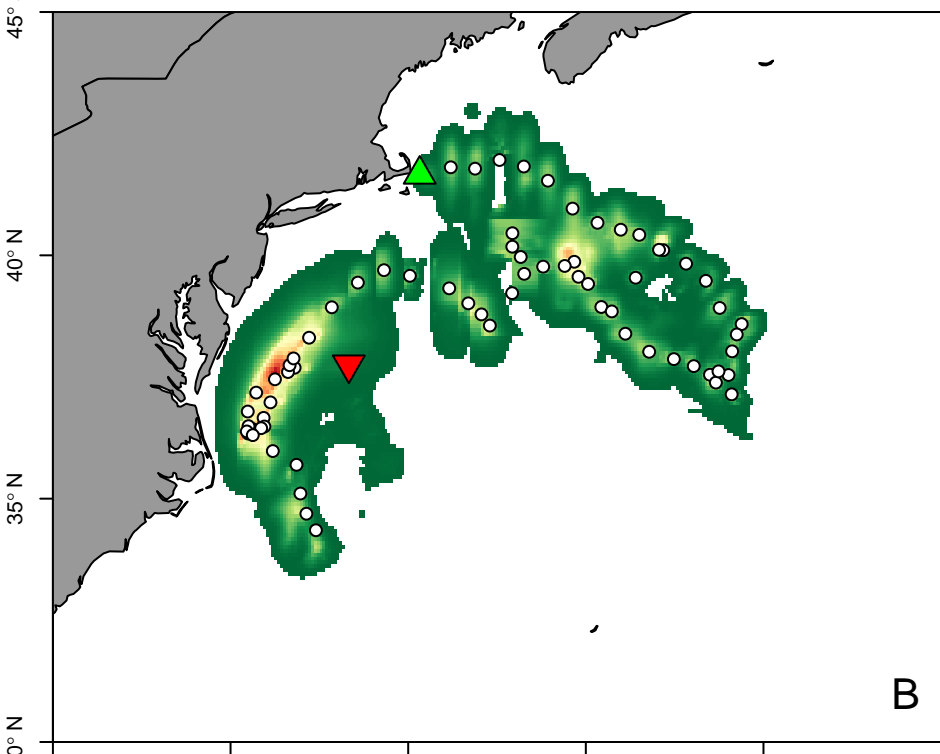
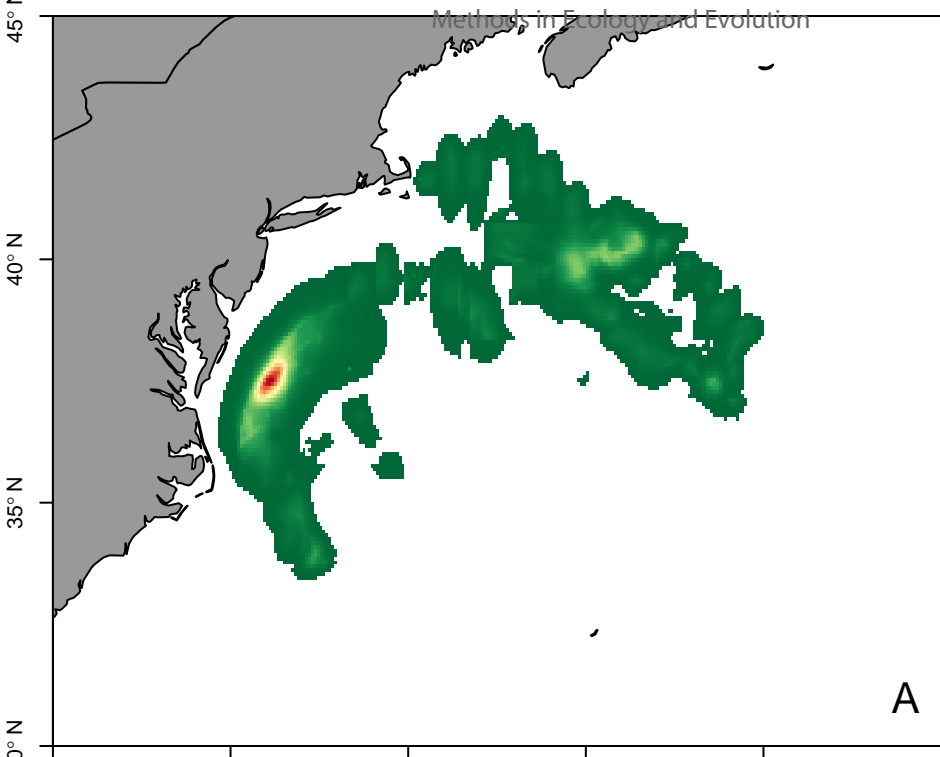
Latitude ($^{\circ}$ N)

B

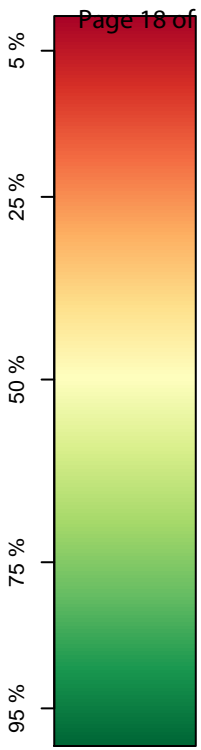
Longitude ($^{\circ}$ E)

C





Expected Proportion of Time Spent



Migratory behavior

Resident behavior